BORDER FAULTS LINKAGE AND SEGMENTATION

ALONG THE MALAWI RIFT

By

HAIFA SALIM AL SALMI

Bachelor of Engineering in Mechanical Engineering

Sultan Qaboos University

Muscat, Sultanate Of Oman

2011

Submitted to the Faculty of the
Graduate College of the
Oklahoma State University
in partial fulfillment of
the requirements for
the Degree of
MASTER OF SCIENCE
December, 2014

BORDER FAULTS LINKAGE AND

SEGMENTATION ALONG THE MALAWI RIFT

Thesis Approved:

Dr. Mohamed Abdel Salam

Thesis Adviser

Dr. Estella Atekwana

Dr. Daniel Laó Dávila

ACKNOWLEDGEMENTS

I would like to express my gratitude to my research supervisor Dr. Mohamed G. Adelsalam for his continuous support to the last day in helping me accomplish my target. He has always been an inspirer a supporter and I was honored to get the opportunity to work with him. I would also like to thank Dr. Estella Atekwana for her inspiration and enthusiasm to always get the best out of me; she has been a parent to me. Thanks also are due to Dr. Daniel Laó Dávila for being in my committee and having constructive comments to enrich my research. I am especially thankful to my mother my father and my two brother for their moral and spiritual support. Not forgetting every single person in my life and my colleagues in school who always support me and encourage me to keep on going. Finally I would like to thank ExxonMobil for provided me this amazing opportunity and for their generosity in providing me a full scholarship to complete my MS degree.

Acknowledgements reflect the views of the author and are not endorsed by committee members or Oklahoma State University.

Name: Haifa Al Salmi

Date of Degree: DECEMBER, 2014

Title of Study: BORDER FAULTS LINKAGE AND SEGMENTATION ALONG THE MALAWI RIFT

Major Field: GEOLOGY

Abstract:

Border fault segmentation characterizes nearly all continental rift zones during their early stage resulting in discrete basins that form the rift system. How border faults form and evolve through time remains a subject of much interest in the study of continental rifts. This study uses Shuttle Radar Topography Mission (SRTM) Digital Elevation Model (DEM) data and previously published seismic sections to investigate the along strike variability in border faults and linkages along the Malawi rift. The availability of SRTM-DEM data allowed detailed examination vertical distance, relationship between basement structures and border fault segments than was previously possible. Detailed topographic profiles were extracted from the SRTM-DEM data at a spacing of 1.4 km along the entire length of the Malawi rift to determine the fault scarp vertical distance. Additionally, seismic cross-sections were used to provide the subsurface structure and displacement of the border faults. The results show the following: (1) Eight border fault segments were identified from the surface data, with segments length varying from ~230 to ~45 km. The general trend observed reveals a decrease in scarp vertical distance from ~2 km in the north to ~0.2 km in the south, confirming the southward propagation and younging of the rift. (2) Unlike the typical cross fault rift model, irregular shaped segments in the Malawi rift show along-strike segmentation by changing from half-graben to full-graben geometry. A half-graben with specific polarity changes to a full-graben geometry before giving place to another half-graben with opposite polarity. (3) Zones of segmentation coincide with pre-existing structures (Permo-Triassic grabens) that strike at high angle to the trend of the rift inhibiting the fault from further propagating. (4) In some cases border faults follow the general structural grain of the basement but deviate from basement structures, striking the later at high angles. (5) Transfers between border fault segments are characterized by conjugate convergent overlap zones. Unlike the commonly held view of rifts compartmentalize by arcuate/sigmoidal shaped border faults alternating in polarity along strike, the results of this study suggest a more complex pattern of border faults and segmentation along the Malawi rift.

TABLE OF CONTENTS

LIST OF FIGURES

Figure Page

Figure Page

CHAPTER I

INTRODUCTION

Continental rift systems are inter-connected groups of half-graben basins bordered by steep escarpments formed by extensional border faults. In the early rift stage, these border faults accommodate most of the strain, causing asymmetry in the basins (resulting in half-grabens), but become abandoned at later stages of rifting (Ebinger and Casey, 2001). Border fault segmentation is a fundamental manifestation of continental extension (Crossley and Crow, 1980; Zorin, 1981; Cape et. al, 1983; Baldrige et al., 1984; Ebinger et al., 1984; Reynolds and Rosendahl, 1984; Smith and Bruhn, 1984; Bosworth, 1985, Rosendahl et al., 1986, Specht and Rosendahl, 1989). Segmentation causes discrete structural basins to form along the rift resulting in the eventual tectonic segmentation of divergent boundaries. How border faults form and evolve through time remains a subject of much interest in the study of continental rift zones. Morley (1999) describes three variants in the evolution of border faults displacement and propagation which include: (1) maximum displacement at the center of each segment with displacement decreasing towards the tips, (2) variable along strike displacement resulting from linkages of en-echelon fault segments and (3) asymmetric propagation where one tip of a fault segment remains fixed whereas the other tip propagates a long distance.

Typically the dip direction of the main border fault segments alternates in polarity from one basin to another forming ~100 km long segments (Ebinger et al., 1987). In cross sectional view normal to the trend of the rift, displacement seems to be higher on one bounding fault (main

bounding fault), or a system of a few main faults which progress into a low angle detachment fault (Bosworth, 1985). Several models have been used to explain the mode of alternation and the array of structures produced as the border faults vary in displacement along a segment and interchange from one segment to the other (Ebinger et al., 1987, Specht and Rosendahl, 1989). These changes in polarity of the basins are connected through a variety accommodation zones. For example, Bally (1982) and Gibbs (1984) presents a series of linear faults (in plan view) separated by a strike-slip accommodation zone orthogonal to the border fault, the former as a conceptual model after looking at various rift zones and the latter for the North Sea. An alternate model presented by Chenet and Letouzet (1983) for the Gulf of Suez suggests curvilinear shaped border fault systems transferring from one fault to the other through accommodation zones formed by between en echelon border fault segments. Similarly Reynolds and Rosendahl (1986) describe the fault geometry in the Tanganyika rift as curvilinear fault segments linked through a number of accommodation zones which includes half-grabens facing away from each other and separated by an interbasinal ridge, and half-graben segments interacting tip to tip. Ebinger et al. (1987) also presented a model of fault geometry for the Malawi rift where fault segments are linked through a variety of accommodation zones formed by segments interacting tip to tip, en echelon segments and segments completely overlapping. Specht and Rosendahl (1989) mapped fault segments separated by accommodation zones that are either interbasinal highs or lows characterized by segments linked tip-to-tip, en echelon segments, and segments completely overlapping. Hence the transition zone between segments is complex and can be represented by different style of accommodation.

The primary objective of this study is to further enhance our knowledge on the geometry of the border faults bounding the Malawi rift, accommodation zones linking individual segments and examining the possible influence of pre-existing structures on border fault segmentation. The Malawi rift (Figure 1) is an ideal place to analyze border fault characteristics, since it displays a

network of basins along its length and previous studies suggest the rift is propagating from north to south with maximum extension rates in the north (Figure 1, Calais et al., 2006, Stamps et al., 2008). This allows for the evaluation of the temporal evolution of the border fault system.

Previous models have utilized gravity and magnetic data covering the western side of the rift acquired by the Malawi Geologic Survey (1985). Aeromagnetic data covering the western side of the rift and the southern tip made available by the Malawi government. Seismic data covering the western side of the rift. Whereas later studies utilized seismic data acquired by project probe (Specht and Rosendahl, 1989). The only satellite imagery used were Landsat-5 Thematic Mapper covering the area between the Rungwe volcanic province and the tip of the Malawi rift. Newly available data such as SRTM-DEM data provides an unprecedented view of the geomorphology of the rift basin allowing us to examine in greater detail the along strike variability of the border faults and linkages than has previously been possible.

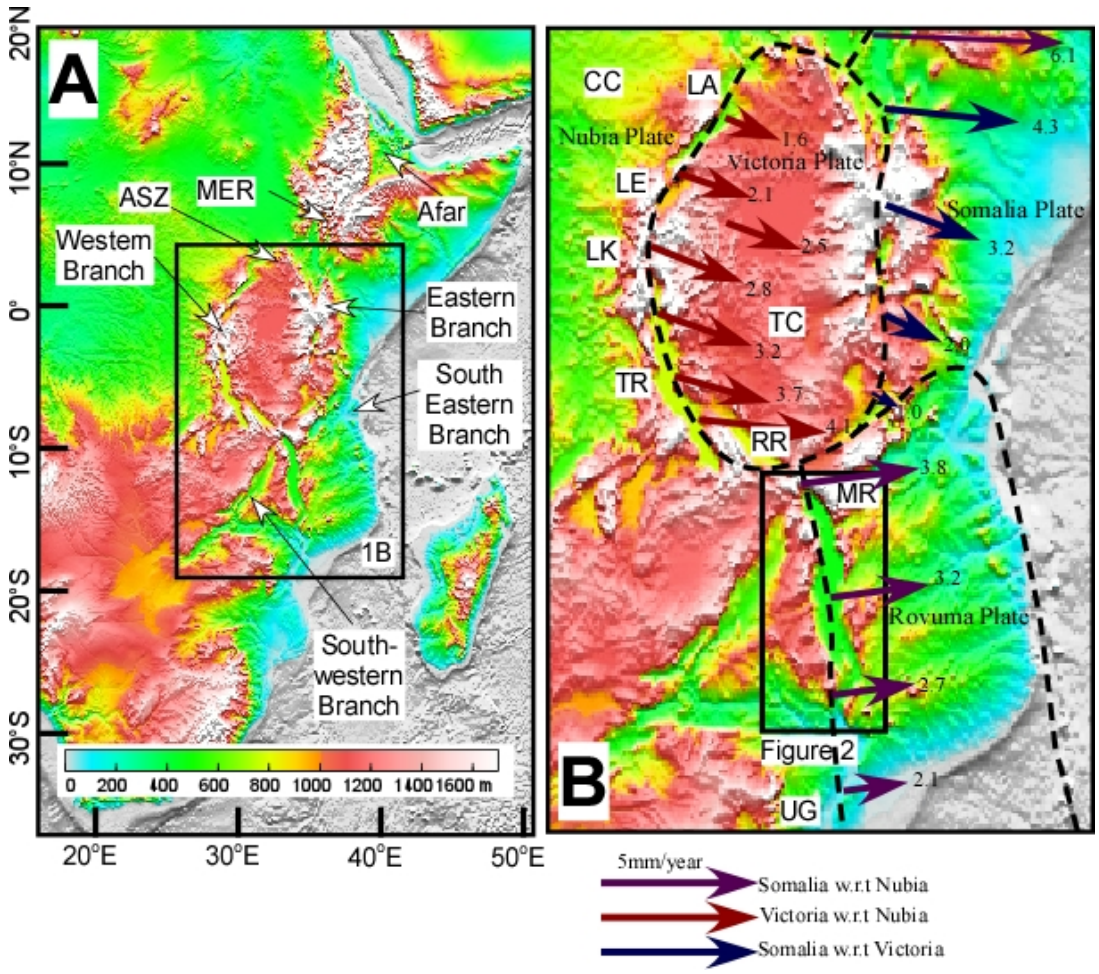

Figure 1: Global 30 Arc Second Elevation Data (GTOPO30) Digital Elevation Model (DEM) showing the East African Rift System (EARS) (A) and the Eastern and Western Branches of the EARS (B). MER = Main Ethiopian Rift. ASZ= Aswa Shear Zone. CC= Congo Craton. LA=Lake Albert. LE=Lake Edward. TC=Tanzanian Craton. RR=Rukwa Rift. MR=Malawi Rift.UG=Urema Graben. Modified after (Calais et al., 2006, Stamps et al., 2008).

CHAPTER II

TECTONIC SETTING

II. I East African Rift System

One of the most remarkable features in Africa is the East African Rift System (EARS) (Figure 1A). From the surface the EARS appears as a long succession of individual tectonic basins (rift valleys) extending for more than four thousand kilometers, bordered by uplifted shoulders and separated by shoals (Figure 1A). Graben valleys are located over major failures in the lithospheric mantle, and appear as major border faults on the surface and transfer into a low angle detachment fault at depth demonstrating a rollover asymmetric pattern (Chorowicz, 2005). The EARS starts from the Afar Depression in Ethiopia in the north, and continues south as a single rift represented by the Main Ethiopian rift before it encounters the thick lithosphere of the Tanzanian craton where it bifurcates into the Eastern and Western Branches (Figure 1A and 1B). The two branches wrap around the thick lithosphere of the Archean Tanzania craton following Proterozoic orogenic belts (Figure 1; Ring and Betzler, 1995). A third, south-eastern branch is also defined in the Mozambique channel formed by the N-striking undersea basin located on the west of the Davie ridge (Chorowicz, 2005). Although it appears as an extension to the Western branch, a south-western branch is also identified south of the western branch, which comprises the Mweru, Luangwa, Kariba, and Okavango rift basins (Chorowicz, 2005; Modisi et al., 2000) (Figure, 1A).

II. II The Western Branch:

The Western Branch extends between the Tanzanian craton in the east and the Congo craton to the west. It extends over a distance of ~2100 km starting from Lake Albert (Mobutu) in the north, to Lake Malawi (Nyasa) in the south. Despite the low volcanic activity in the Western branch, it is seismically active along its entire length. In the north, the branch terminates against the NW-trending Precambrian sinistral strike-slip Aswa Shear Zone (Katumwehe, 2013). The northern segment includes Albertine, Edward and Kivu basins. The central segment includes basins of lake Tanganyika and Rukwa. Finally the southern segment is mainly comprised of Lake Malawi (Nyasa) and the Dombe and Urema grabens in Mozambique (Chorowicz, 2005) (Figure 1B).

Extension of the Western Branch is explained by kinematics of the Nubian, Somalian, and the Victoria (Tanzanian) micro plates (Calais et al., 2006). It was developed due to the southeastern motion of the Somali plate and anti-clockwise rotation of the Victoria micro-plate relative to the Nubia plate. GPS data indicate that the EARS is opening at a rate of ~1 to 4 $mmyr^{-1}$ across both the Western and the Eastern branches, increasing from north to south for the Western branch and from south to north for the Eastern branch (Stamps et al., 2008).

II. III Structural Setting of the Malawi Rift:

The Malawi rift is a Cenozoic-aged rift representing the southernmost segment of the Western Branch of the EARS (Figures 1 and 2). The Malawi Rift began subsiding during the late Miocene ~8-9 Ma (Harkin, 1960; Ebinger et al., 1984, 1987, 1989, 1993). However, major rifting in the northern part of the rift initiated at 6-5 Ma, and increased in length southwards (Flannery and Rosendahl, 1990). In the extreme north end of the rift lies the only Cenozoic volcanism associated with the Malawi rift (Rungwe Volcanic Province) (Figure 2). It is associated with the late Miocene-Quaternary Rungwe complex in Tanzania (Bloomfield, 1966; Carter and Bennett, 1973; Ebinger et al., 1989). Although it is suggested to be ~900 km long from the Rungwe

volcanic province (Tanzania) in the north to the Urema graben (Mozambique) in the south (Figure 1B; Ebinger et al., 1987), the part of the rift that is filled by lake Malawi extends ~550 km with a width of ~50 km (Figure 2 and 3). In the northern part of the rift it strikes north-northwest, making it parallel to the regional structural grain of the Paleoproterozoic Ubendian belt and perpendicular to the Mesoproterozoic Irumides orogenic belt (Figure 3). At its southern boundary, the rift meets the Neoproterozoic (Pan-African) northwest-striking Zambezi belt. In the south, the regional structural grain of the Neoproterozoic Zambezi belt is parallel to the eastern margin of the Malawi Rift (Figure 3) (Daly and Quennell, 1986).

The rift is filled with lake Malawi and is bounded by elevated curvilinear border faults that can reach a relief in excess of ~1500 m. The border fault throw is between ~2.5 and ~5 km partitioned between the topographic escarpment and subsurface extension of the fault. The basin's subsidence reflects accumulation of sediments and rift flank uplift, where the water surface is at 474 m above sea level, and the maximum depth is ~700 m (Delvaux, 1995). Extension rates in the Malawi region range from 4.5 $mmyr^{-1}$ in the North to 1.3 $mmyr^{-1}$ in the South (Stamps et al., 2008).

Earlier models proposed for the rift present a curvilinear or an "S" shape geometry formed by opposite concavity segments (Ebinger et al., 1987, Specht and Rosendahl, 1989). Alternation of border fault segment presented by previous models suggests "flip-flopping" of the basinal asymmetric segments produced (Ebinger et al., 1987, Specht and Rosendahl, 1989). Different analyses suggest a different model presenting various number of border fault segments. The first model suggests ten segments (Figure 4) (Ebinger et al., 1987). Ebinger et al. (1987) also suggests that segments have developed diachronously due to variations along-strike in depositional sequences and fault patterns. These difference has been used to divide the rift into five structural provinces along the Malawi rift which include: Karonga, Nkhata, Nkhotakota, Monkey Bay, and Shire. Moreover, Ebinger et al. (1987) concluded no correlation between rift

segmentation and pre-existing structures. A second model suggests seven fault segments (Specht and Rosendahl, 1989). Each segment is named based on the half-graben and include: Livingstone, Usisya, Mbamba, Bandawe, Mantagula, Mwanjage and Mtakataka. A third model suggests nine segments (Rosendahl et al., 1992). This model suggests a correlation between segmentation and Proterozoic Chamaliro dislocation zones (Figure 2). Moreover, the rift was also divided into half-graben segments, which include: Livingstone, Usisya, Mbamba, Likoma, Badawe, Mentangula, Mtanga, Makanjila, and Mtakataka. Finally the fourth model suggests four half-graben units (Versfelt and Rosendahl, 1989, Chorowicz, 2005). It is clear that the segments vary from one interpretation to the other based on the criteria used to define a half-graben segment. Linkages between these faults have been characterized in all the previous models by four main modes. The first is the most popular cross fault rift model (Bosworth, 1985). Rift segments dipping in the opposite direction and facing each other interact tip to tip and do not propagate past each other. The second mode is the en echelon transfer mode. The two segments are dipping in the same direction and are located on the same side of the rift. The third mode is where the two fault segments are dipping in the opposite direction and are connected through a strike-slip fault. The fourth mode is when the two fault segments are completely overlapping each other. Full-graben geometries are only suggested to form in this type of linkage.

The rift traverses a complex array of Proterozoic orogenic belts and Permo-Triassic (Karoo Grabens) and Cretaceous graben systems (Figure 2). Structural province divisions proposed by Ebinger et al. (1984) due to the diachronous development of the various segments of the Malawi rift will be used for the purpose of this discussion (Figure 2). Although the Malawi rift is bounded by fault systems from north to south only a few have been named. The most pronounced fault system in the Malawi rift is the ~120 km long Livingstone fault located on the eastern side of the rift at the northern tip (Figure 2). Also the Koronga fault in the north part of the rift in the Koronga province ~50 km form the Rungwe volcanic province, which extends for a

length of ~17.8 km (Biggs et al., 2010). This fault is associated with the 2009 earthquake and is declared a natural disaster area by the government (Biggs et al., 2010). Another fault is the three step ~200 km long Usisya fault system located in the center of lake Malawi (Figure 2) (Contreras et al., 2000). Followed by the Bilila-Matakataka fault which is ~125 km and located on the western side of the rift at the southern end of lake Malawi (Figure 2) (Jackson and Blenkinsop, 1997). Finally the last identified major fault on the rift is the insufficiently studies NW striking transform Mwanza fault in the southern end of Malawi rift in the Shire province (Castaing, 1991).

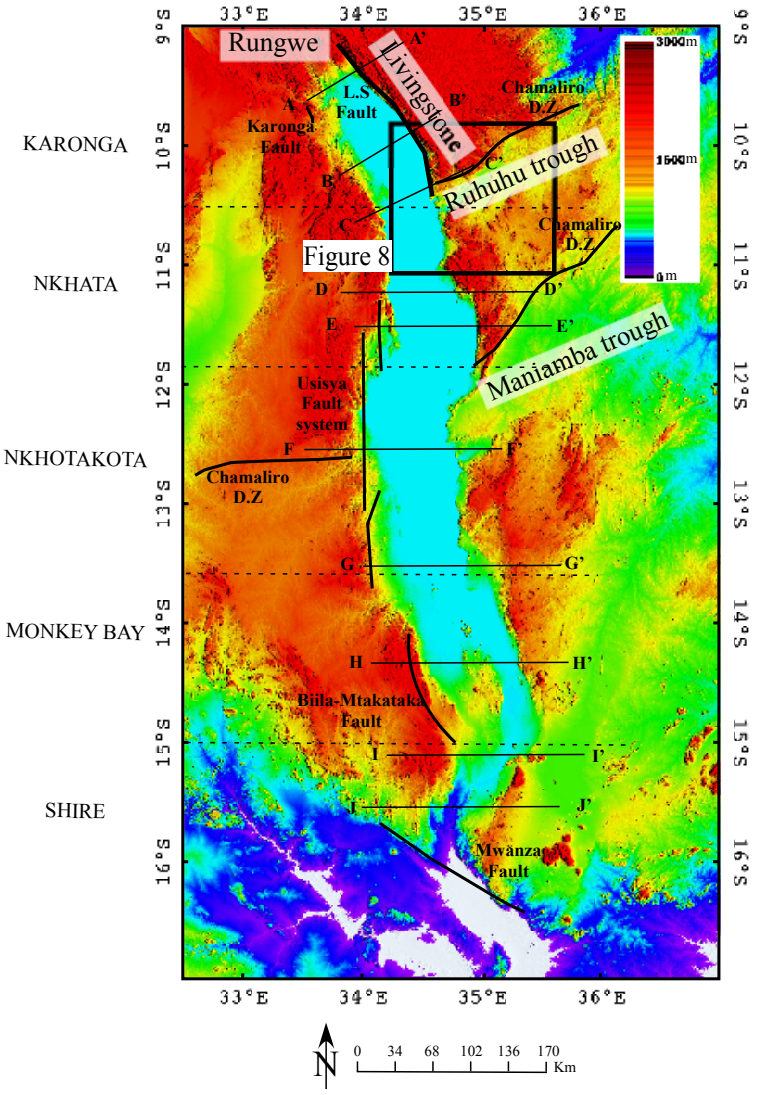

Figure 2: Shuttle Radar Topography Mission (SRTM) Digital Elevation Model (DEM) of the Malawi rift. Cross section profiles are shown in Figure 5.

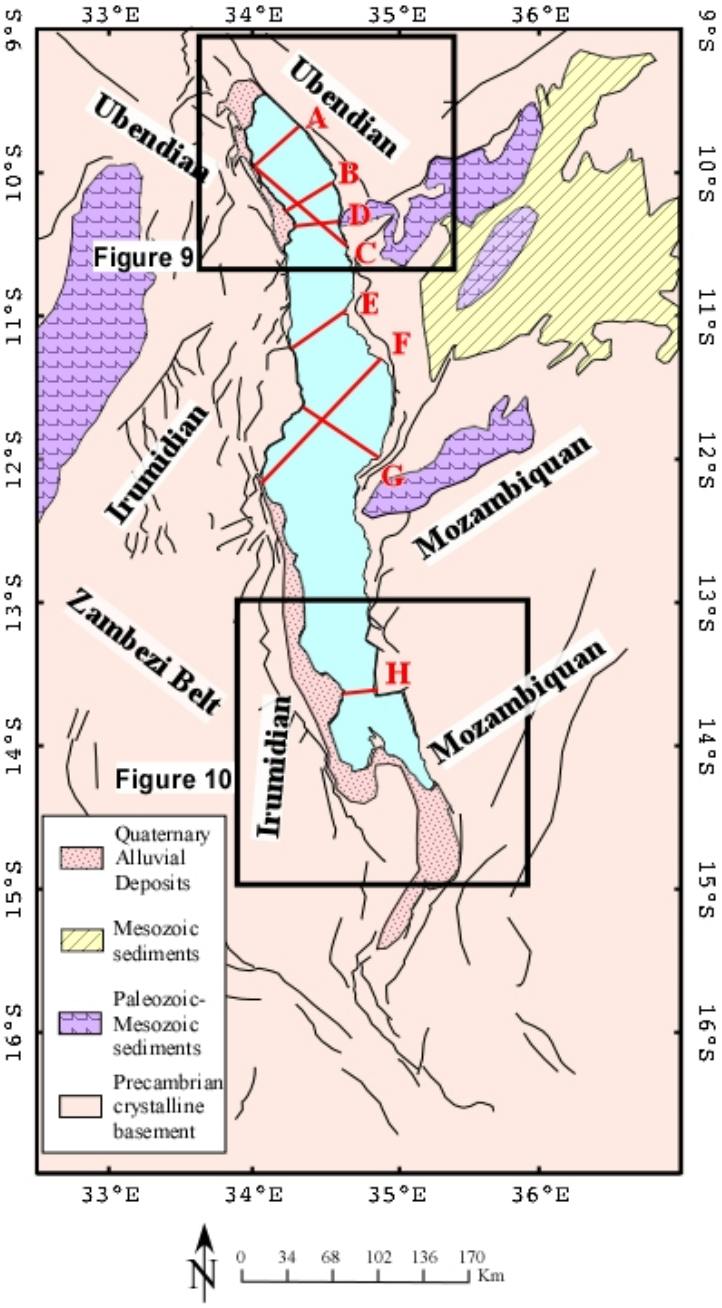

Figure 3: Geological map of the Malawi rift and surroundings. Ubendian, lrumidian, and Mozambiquan refer to tectonic provinces associated with Proterozoic to Precambrian orogenies that affected this region. Surface geology is modified from the International Geological Map of Africa 1:5,000,000 scale, Third Edition 1985-1990; a co-publication of CGMW/UNESCO with financial support from PRGM. Transect sections show locations for Figure 6.

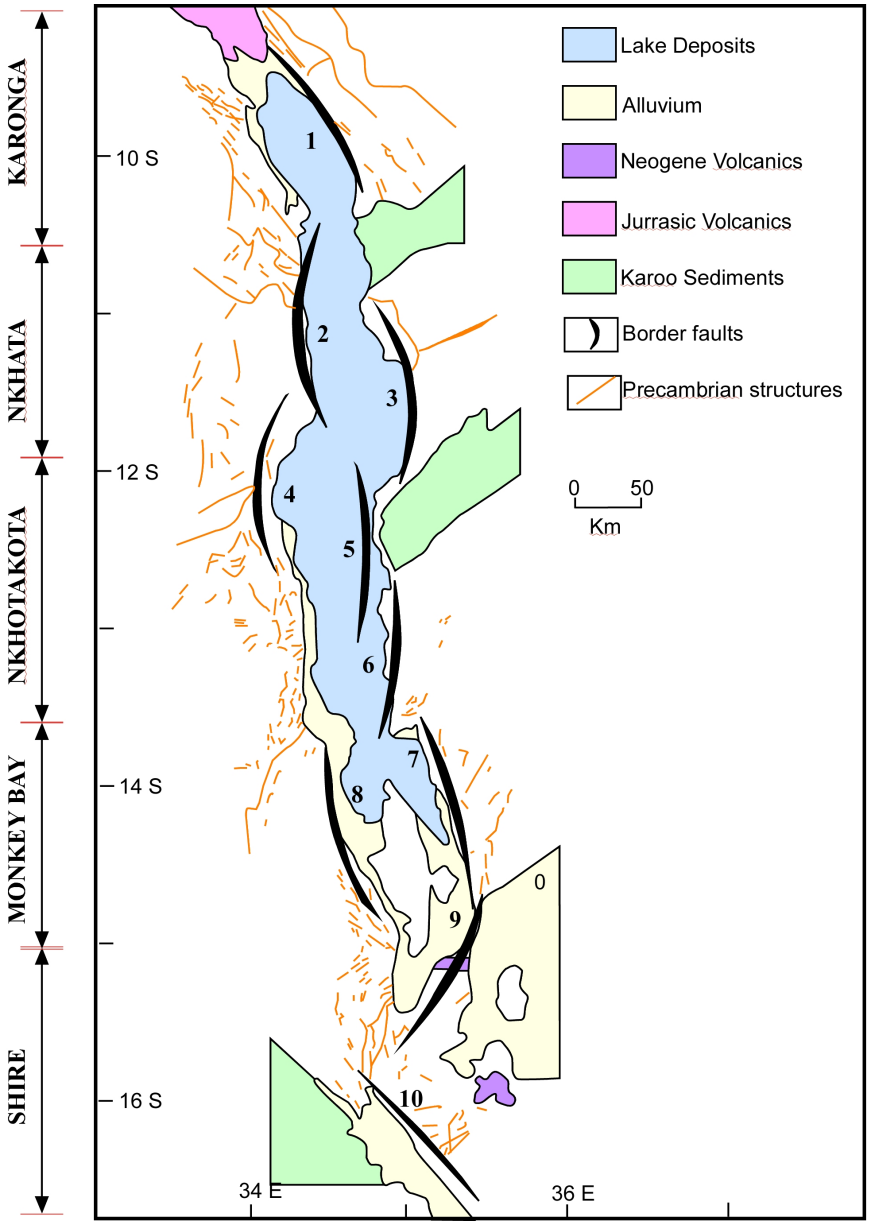

Figure 4: Tectonic map of the Malawi rift showing the underlying preexisting structures and the extent of the rift segments. Modified after (Ebinger et al., 1987).

CHAPTER III

DATA AND METHODS

III. I SRTM data analysis

Shuttle Radar Topography Mission (SRTM) is classified as the only spaceborne single-pass interferometric Synthetic Aperture Radar (SAR) imaging system. SRTM was an international joint project collected in February 2000 by the United States National Geospatial-Intelligence Agency (NGA) the National Aeronautics and Space Administration (NASA), and the German and Italian Space Agencies. SRTM DEM is distributed by NASA's Jet propulsion lab (JPL) in 1° × 1° tiles. Available types of SRTM are: one arc data (SRTM-1, 30m X-Y resolution); and three arc data (SRTM-3, 90m X-Y resolution and ±30m root mean square error z accuracy). SRTM-3 is the only available data for Africa and hence the dataset used in this study. SRTM DEM data were analyzed using a software for processing and analyzing spatial imagery called Environment for Visualizing Images (ENVI). A mosaic was formed by combining data scenes and registered using image-to-image techniques (Chen and Lee, 1992).

Topographic profiles were extracted perpendicular to the rift direction, at approximately 1.4 km spacing along the whole length of the rift lake. These profiles contain z-values, which represent the vertical distance of the escarpment (Figure 5). In some areas Lake Malawi marks the eastern and western bounds of the rift, hence the eastern and the western border faults correspond to the edges of the lake. However in other areas border faults are beyond the edge of the lake. Values of the east and west vertical distance of the border faults were plotted against their

location from north to south. Smoothing of the data was performed by local regression using weighted linear least squares and a second degree polynomial model. Critical information was extracted from the plot. This includes vertical distance of escarpment, number of segments along the rift, length of the border fault segments, mode of linkage, style of accommodation, polarity of the structure formed, locations of full-grabens, general trend of vertical distance from east to west, and potential location of rift termination. Border faults were then identified based on the vertical distance profile across that area which determines if the fault is a master border fault or just a minor fault. Profiles clearly showed which fault has the higher vertical distance and hence representing the mater border fault. In the case of the half-graben, one border fault accommodates most of the vertical distance and subsurface displacement while the other boundary does not have a well developed border fault and remains as a hinge zone, which can be referred to as a rollover fold. On the other hand, a full-graben is expected to have almost equal vertical distance and subsurface displacement on both border faults bounding it. Each segment has minimum displacement at the tips and maximum in the middle and represents a half graben. This was the criteria used to identify the segments. Segments lengths were identified based on the distance measured as a transect from north to south . Values plotted in the Y-axis represent the vertical distance for each segment. Scarp height was used as a proxy for vertical distance. A segment having a higher vertical distance on the east escarpment dips to the west, and a segment having a higher vertical distance on the western escarpment dips to the east.

In addition, the SRTM data was processed using Geosoft's Oasis Montaj software system. Several edge enhancement filters (including derivative, analytical signal, tilt derivative) typically used for enhancing shallow structures in gravity and magnetic data were applied to the SRTM. The produced X-derivative map was then used to map the border fault segments and basement structures based on abrupt changes in color, and tonal patterns. Master border faults had a higher rank (based on color) in the derivative scale and so were identified from minor faults. These faults were then compared to the border faults obtained from the plot extracted from the

SRTM DEM data.

III. II Seismic data analysis

STRM provides information on the surface morphology of the faults. To determine the subsurface variation of the faults, fourteen multifold seismic reflection profiles acquired as part of Project PROBE and available in the published literature (Specht and Rosendahl, 1989) were digitized using Canvas. These sections only cover the lake section of the rift and were acquired in time and converted into depth sections using the 3:1 vertical exaggeration scale provided in the literature (Specht and Rosendahl, 1989). Seismic data were used to map the subsurface continuation of the border faults displacement, their geometries and associated dip directions using the same criteria used for the surface (Figure 6). Rosendahl et al. (1992) presented line drawings of seismic sections exceeding in number the sections presented by Specht and Rosendahl (1989). Although those line drawings presented by Rosendahl et al. (1992) were in time and could not be converted into depth they were utilized to obtain major observations on subsurface geometry and dip directions. Length of the segments were obtained from the line drawings aided by the subsurface geometry showing the transfer from segment to the other. Approximate lengths were measured based on the locations where the line drawing were obtained. Measurements were made from a north-south transect from the northern tip of segment 1.

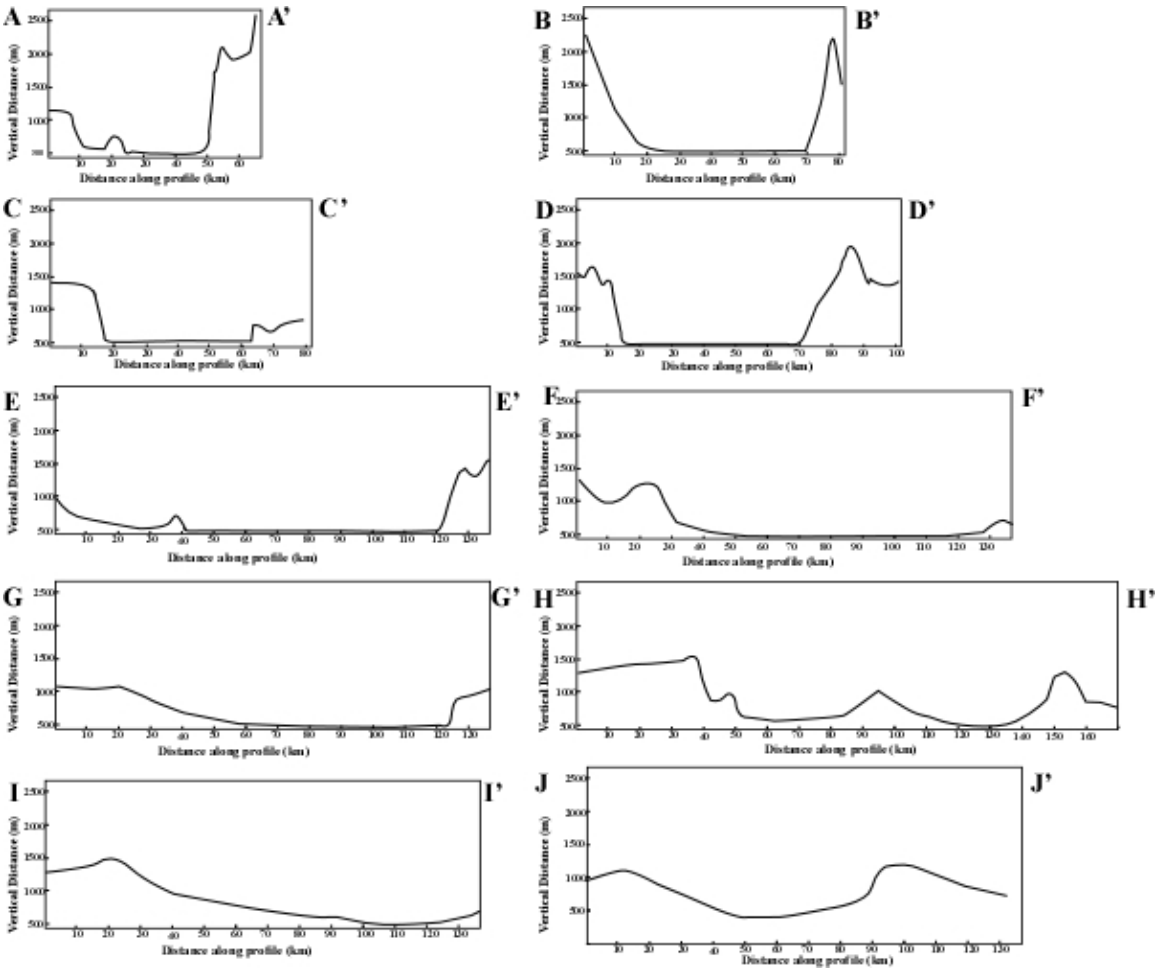

Figure 5: Examples of profiles mapped at several locations across the rift showing different geometries profile locations are shown in Figure 2.

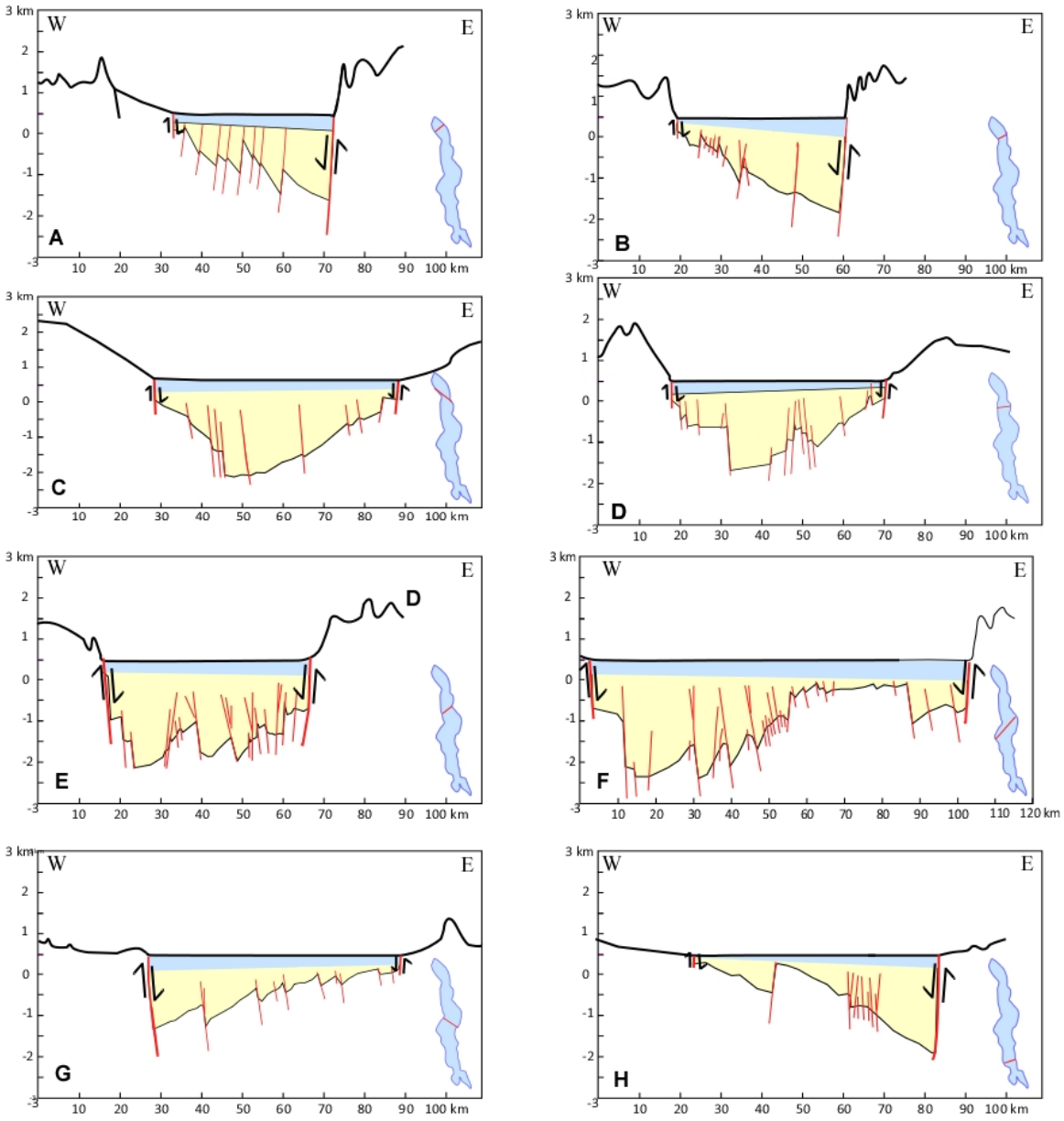

Figure 6: Representative visual interpretation of Seismic sections collected across the Malawi rift by Specht and Rosendahl (1989) (Vertical Exaggeration 3:1), integrated with topographic profiles along the same base line from SRTM DEM. Inset maps of Lake Malawi show the orientation of each transect.

CHAPTER IV

RESULTS

Border fault length and vertical distance is summarized in Figure 7 (from the 1.4 km spacing profiles extracted from the SRTM), which shows the east and west fault scarp vertical distance versus distance along the length of the Malawi rift extending from north to south and Figure 5 shows example profiles. The SRTM data suggests the following: (1) Eight border fault segments (marked on Figure 8) that vary in length from a maximum of ~230 km at segment two and five to a minimum of ~45 km at segment seven and eight in the South. All the lengths were measured from a north-south transect from the start of segment one. Segment one extends from the northern tip of the Malawi rift to ~130 km. The eastern border escarpment starts with a high vertical distance of ~2 km while the western escarpment starts from ~1.2 km (Figures 5 (A-A') and 7). Both escarpments then decrease abruptly and level off at ~25 km from the tip. The eastern escarpment reaches to a vertical distance of ~0.8 km, while the western escarpment reaches a vertical distance of ~0.65 km suggesting a difference in escarpment of ~150 m. This segments presents a west dipping half-graben since the eastern escarpment has a higher vertical distance (~0.8 km) than the western escarpment (~0.65 km). At ~ 125 km across both the eastern and the western escarpments have a vertical distance of ~0.8 km. This represents the formation of a full-graben (Figures 5; B-B'). Segment two extends from ~50 km to ~280 km extending for 230 km. After the formation of the full-graben the western escarpment increases in vertical distance to reach a peak of ~1.2 km, whereas, the eastern escarpment decreases in vertical distance to reach a minimum of ~0.55 km. This location presents the formation of half-graben dipping to the east

with a difference in escarpment vertical distance ~0.65 km between the east and west of (Figure 5; C-C'). Once a half-graben is reached both the escarpments behave oppositely to reach the same displacement and present a full-graben geometry (Figure 5; D-D'). This transfer in geometry from a half-graben to a full-graben followed by a half-graben of the opposite polarity is repeated throughout the following segments. Segment three begins at ~160 km and ends at ~330 km extending for 170 km. Both the east and west escarpments decrease in vertical distance to reach a minimum of ~0.9 km and ~0.6 km respectively, this segment presents a west dipping half-graben (Figure 5; E-E'). Both escarpments then increase in vertical distance to reach ~1 km and form a full-graben. Segment four extends from ~300 km and ends at ~400 km extending for 100 km and presenting an east dipping half-graben (Figure 5; F-F'). The western escarpment reaches a maximum of ~1.2 km and then decreases to reach ~0.6 km, while the eastern escarpment decreases in vertical distance from ~1 km to ~0.6 km, where they form a full-graben. The maximum difference in scarp vertical distance between the two is ~0.3 km. Segment five extends from ~370 km to~600 km extending for 230 km and presents a west dipping half-graben. Where the east escarpment has a maximum vertical distance of ~0.9 km and the western escarpment has a minimum of ~0.6 km and the maximum difference in scarp vertical distance between the two is ~0.3 km. A full-graben is then formed with a vertical distance of ~0.8km (Figure 5; G-G'). Segment six extends from ~475 km to ~650 km extending for 175 km. Unlike the other segments, segment 5 doesn't segment after the formation of the full-graben; it continues to overlap with segment 6. Both the east and the west escarpment increase in vertical distance, the west escarpment has a maximum of ~1.1 km, and the east escarpment increases from ~0.6 to ~1 km. The rift then bifurcates into two basins, an eastern and a western basin and accordingly we have both an east and a west border fault (Figure 5, H-H'). Segment 5 then terminates at ~600 km and segment six forms an east dipping half-graben (Figure 5; I-I'). Segment seven extends from ~625 km to ~670 km extending for 45 km and presenting a west dipping half-graben. Both the east and west escarpments decrease in vertical distance abruptly to reach ~0.2 km where they form a full-

graben (Figure 5, J-J'). Finally segment eight extends from ~655 to ~700 km extending 45 km and presenting an east dipping half-graben with a maximum vertical distance of ~0.5 km (Figure 5;). The western escarpment has a slightly higher vertical distance (~0.3 km) than the eastern escarpment (~0.2 km). The general trend observed reveals a decrease in vertical distance of escarpment from ~2 km in the North to ~0.2 km to the South (Figure 7).

Seismic data suggests that the first segment extends for ~125 km from the North and shows a west dipping half-graben geometry with displacement increasing from ~1.5 km to ~2.5 km on the eastern border fault (Figure 6 A and B). This half-graben segment is called the Livingstone half-graben. Following is a full-graben geometry with a displacement of ~2.5 km (Figure 6 C). Next is segment two extending for ~220 km dipping to the east and identified as the Usisya half-graben unit. Following is a full-graben geometry increasing in displacement from ~0.5 km to ~2.5 km (Figure 6 D and E). Segment three then shows a west dipping half-graben and extends for ~170 km corresponding to the Likoma half-graben. A full-graben geometry is then followed by that with a displacement of ~1.5 km (Figure 6 F). Following is a segment four which extends for ~100 km dipping to the east with a displacement of ~1.5 km and corresponds to the Bandawa half-graben (Figure 6 G). A full-graben geometry is then observed at the end of segment five. Segment five then extends for ~80 km, and dips towards the west with a displacement of ~2.5 km representing the Metangula half-graben (Figure 6 H). Segment six, and seven extend for 30 km and 40 km respectively. Both segments represent west dipping half-grabens corresponding to the Mtanga and the Makanjila half-graben respectively. The final segment represents the Mtakataka half-graben and extends for ~10 km dipping also dipping towards the west. Segments six, seven and eight all dip in same direction and as segment five and so they can all be summed into a one segment (Segment five) and not four separate segments. Hence segment five represents a west dipping half-graben and extends for ~160 km to cover part of the Monkey bay province . Formation of full-grabens at the end of each segment is consistent

with observations at the surface (Figure 5 and 6). The naming of the last three segments was then adapted to segment six, seven and eight that extend beyond the lake.

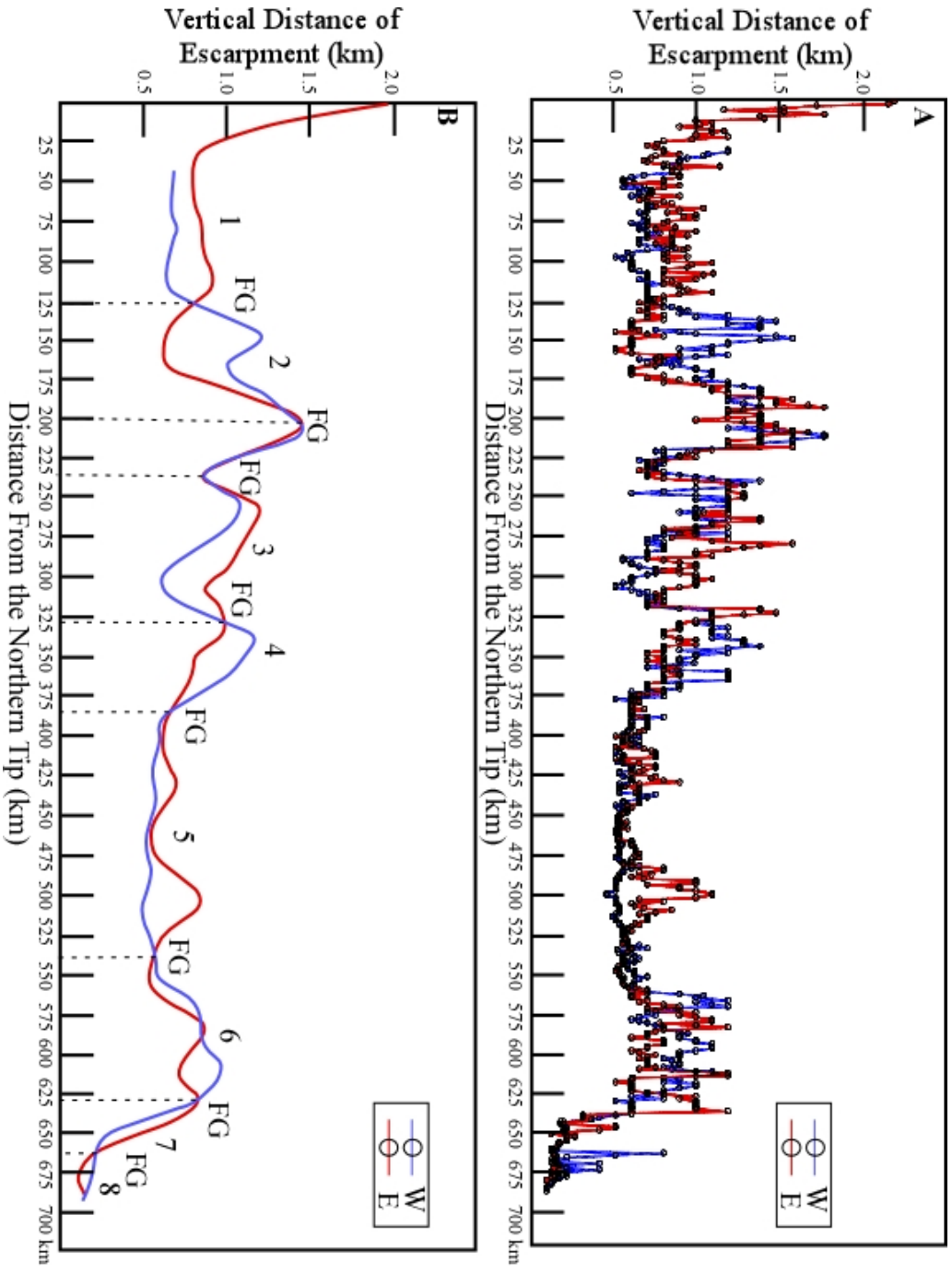

Figure 7: (A) Escarpment vertical distance of the Malawi rift extracted from Shuttle Radar Topography Mission (SRTM) Digital Elevation Model (DEM) sampling interval of 1.4 km on EW profiles. (B) Smoothing of the original data to avoid misrepresentation of the escarpment vertical distance due to mass wasting FG=Full-graben.

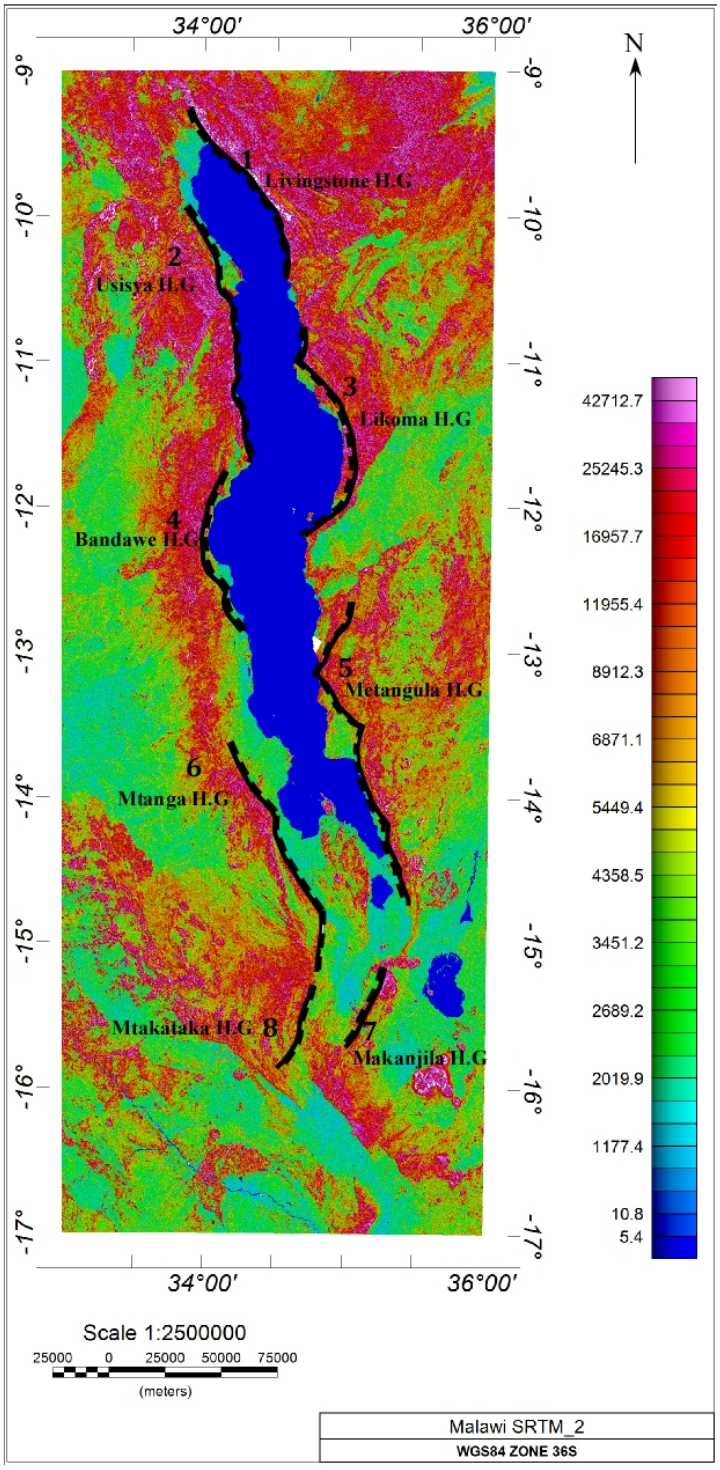

Figure 8: Shuttle Radar Topography Mission (SRTM) Digital Elevation Model (DEM) of the Malawi rift showing the extent of the proposed rift segments.

(2) Zones of segmentation coincide with regions where the pre-existing structures (Permo-Triassic grabens) strike at high angle to the trend of the rift (Figures 2 and 9). Two Permo-Triassic Grabens Ruhuhu trough and the Maniamba trough trending SW at a high angle to the eastern border fault system of the Malawi rift (Figure 2). The Ruhuhu trough interferes with the end of segment one, forming a barrier and preventing the Livingstone fault from further propagating. Similarly the Maniamba trough trends SW at a high angle to the trend of the rift specifically at the end of the third segment. Suggesting the interference of the Maniamba trough and inhibiting further propagation of the fault . Moreover, it suggests the possibility of the zone deflecting or modifying the strain field in the upper crust causing strain localization and termination of the fault segment.

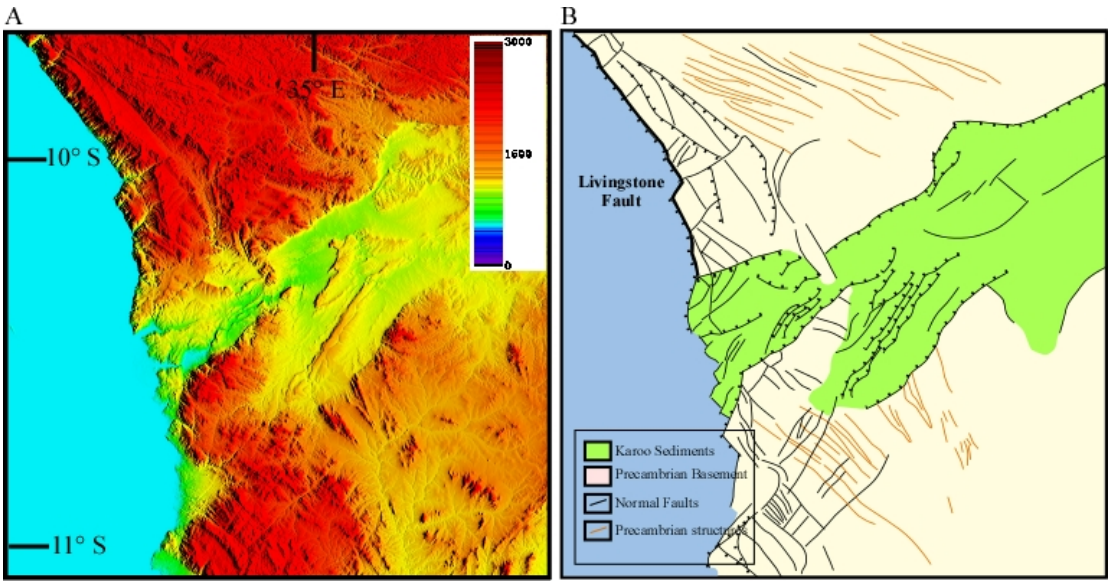

Figure 9: (A) SRTM DEM showing the segmentation of the Malawi Rift at its intersection with the Pre-Existing structure of the Karoo Rift. (B) Structural interpretation of the SRTM DEM showing the segmentation of the Malawi Rift at its intersection with the Pre-Existing structure of the Karoo Rift.

(3) In some cases border faults follow the general structural grain of the basement but deviate from basement structures, striking the later at high angles in other cases (Figure 10 and 11). Basement structures bordering the Livingstone fault (Segment 1) trend in the same NW direction to the trend of the rift (Figure 10). Basement structures are also observed to strike the border fault

at an angle. Figure 11 provides an example of Precambrian structures trending NE at a high angle to segment six, suggesting that the orientation of Proterozoic basement structures relative to the active principal stresses determines the potential of reactivation.

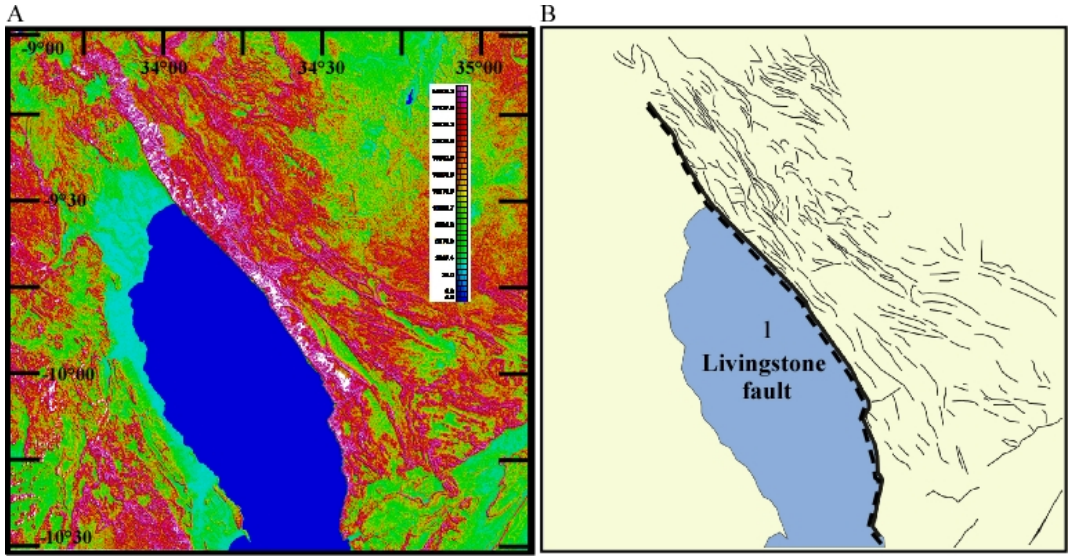

Figure 10: (A) SRTM DEM showing the Livingstone fault trending parallel to Preexisting Precambrian structure. (B) Structural interpretation of the SRTM DEM showing the Livingstone fault trending parallel to Preexisting Precambrian structure.

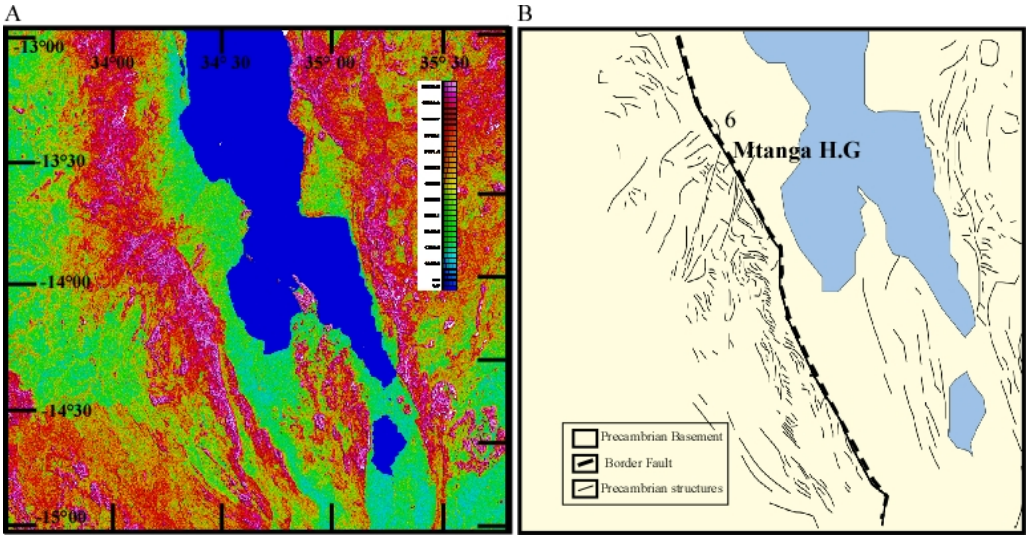

Figure 11: (A) SRTM DEM showing an example of segment 6 not following Preexisting Precambrian structure. (B) Structural interpretation of the SRTM DEM showing an example of segment 6 not following Preexisting Precambrian structure.

(4) Transfers between border fault segments are characterized by conjugate convergent overlapping transfer linked through interference accommodation zones. Half-graben segments in the Malawi rift are formed by the overlap of two consecutive half-graben segments dipping inwards towards each other in the opposite direction to form a conjugate overlapping transfer forming an interference accommodation zone characterized by a full-graben (Figure 12). For example, in segment 1 the eastern border fault has a higher vertical distance (0.9km) than the western border fault (0.7km) (Figure 7). However, the western border fault has a significant vertical distance (0.7km) compared to the eastern border fault. Moreover, the increase in vertical distance of the western border fault indicating the start of the second segment begins approximately half way through segment 1. Unlike a Conjugate Convergent approaching transfer where one border fault has a significantly higher vertical distance compared to the other and the second segment only start to increase in vertical distance near the end of the first segment (Figure 12). Moreover, this geometry as opposed to the synthetic en echelon is indicative of the propagation of border faults through hard linkage.

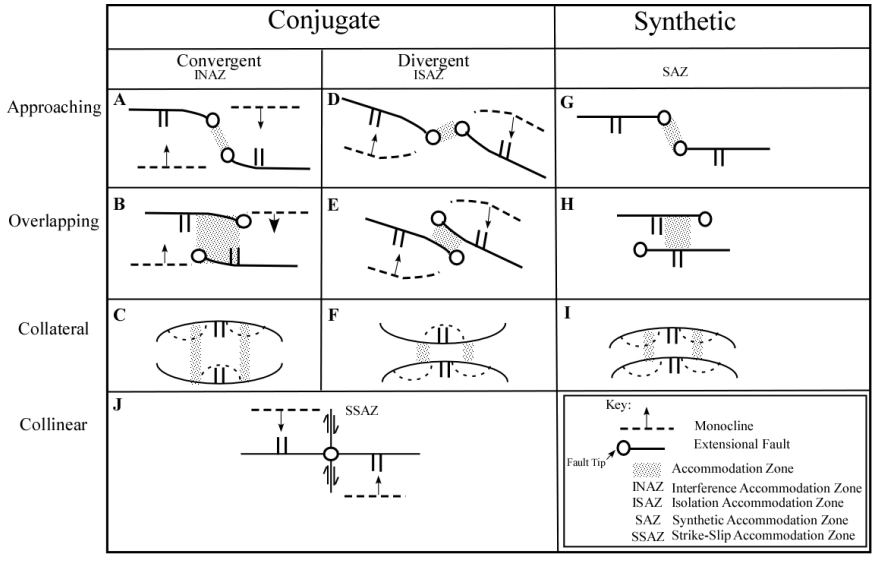

Figure 12: Visual representing different fault linkage transfers: (A) Conjugate Convergent Approaching (B) Conjugate Convergent Overlapping (C) Conjugate Convergent Collateral (D) Conjugate Divergent approaching (E) Conjugate Divergent Overlapping (F) Conjugate Divergent Collateral (G) Synthetic En Echelon approaching (H) Synthetic En Echelon Overlapping (I) Synthetic En Echelon Collateral (J) Conjugate Convergent/Divergent Collinear. Modified after (Morley et al., 1990).

CHAPTER V

DISCUSSION

V. I Border fault segments length, escarpment vertical distance from surface and displacement from subsurface data

Our results show a different pattern than that observed previously in literature. Eight segments were identified from the along strike segments and the seismic data (Figure 7). Each segments starts at the low point and increases to reach a maximum vertical distance and then decreases again to reach a point where the vertical distance is equal to the escarpment on the opposing side of the rift. This in the graph is where the two curves intersect which identifies the location of a full-graben. The segment continues to decreases again to a low point. The next segment starts before the location of the full-graben, specifically where the previous segment was at its maximum vertical distance. The segment continues in the same trend and ends after the formation of the next half-graben. Segments one to eight correspond to: Livingstone, Usisya, Likoma, Badawe, Mentangula, Mtanga, Makanjila, and Mtakataka half-grabens. The trend shows a variation in the length from a maximum of ~230 km in segment two and five to a minimum of ~45 km in segment seven and eight Clearly the length of segments are consistent from the two data sets (SRTM DEM and seismic). The only major difference in length occurs in segment 5, and that is due to the limitation of the seismic data to cover only the portion of segment five covered by the lake. However, lengths obtained from the subsurface data are only

approximations based on the limited available profiles which are at a very high separation. Lengths of the segments and the number of segments are consistent from both data sets.

The trend also shows a decrease in displacement from ~2 km in the North to ~0.2 km in the South as shown by the surface data (Figure 7). Although we had a limited number of subsurface profiles these profiles show that vertical distance from the surface extended to the subsurface and a somewhat consistent high displacement in the basin. Which can indicate the surface topography being affected by mass wasting and other erosive processes. As observed from the Malawi rift, both full and half-grabens characterize the structure of the rift. A half-graben with specific polarity changes to a full-graben geometry before giving place to another half-graben with opposite polarity. Hence, half-graben and full-graben geometries are described as end members. In the case of the half-graben one border fault accommodates most of the vertical distance and displacement while the other boundary does not have a well developed border fault and hence remains as a hinge zone, which can be referred to as a rollover fold. On the other hand, a full-graben is expected to have almost equal vertical distance and displacement on both border faults. However, the plot of the SRTM DEM data (Figure 7) shows that there is a whole array of rift geometries between a full-graben and a half-graben where vertical distance/displacement of different magnitudes is observed at both border faults.

Decrease in vertical distance from North to South is an indication that the border faults are less developed in the South compared to the North. GPS data presented by Stamps et al. (2008) indicate that extension across the Malawi rift decreases from 4.5 $mmyr^{-1}$ to 1.3 $mmyr^{-1}$ in the South at the Mozambique costal plain. Hence suggesting that the rift is younging to the south. This supports our data since both the vertical distance and length of segments are decreasing to the south.

V. II Possible influence on Zones of segmentation

Zones of segmentation of two border faults on the eastern Malawi rift coincide with regions where Permo-Triassic Karoo grabens are at high angle to the trend of the rift (Figure 8). This points out that further propagation of major border faults segments one and three was prevented by the Ruhuhu and the Maniamba Troughs. Permo-Triassic graben zones were not reactivated by the rifting event these structures were able to modify the strain field in the upper crust (Rosendahl et al., 1992), and cause the border faults to segment and alternate sides to avoid these stronger units. Permo-Triassic karoo graben reactivated by the rifting event would portray the pattern observed in the Rukwa Rift. Where Permo-Triassic karoo grabens surround the boundaries of the rift and act like a boundary between extended and non extended terranes indicating that the zone was reactivated by the rifting event (Rosendahl et al.,1992). Not all border fault segmentation is caused by Karoo grabens. However, all Karoo graben locations intersect with border fault segmentation. Segmentation of the other border faults in the eastern and western boundary of the rift do not appear to be associated with any interference from preexisting structure. Cessation of activity is more prolonged and caused by the restriction of the displacement to narrow areas of the fault causing border fault segmentation (Morley, 2002).

V. III Precambrian Basement structure

The role of Precambrian structures was also studied. Border fault seems to trend in the Same NW direction of preexisting Precambrian structures in some locations giving the example of the Livingstone border fault (Figure 9). However, in some locations preexisting basement structures seem to trend at a high angle to the trend on the border fault (Figure 10). Border faults appear to be trend irrespective of the trend in preexisting Precambrian basement structure. A possible explanation for the variation in trend of the Precambrian structures relative to the trend of the border faults may be the pre-rifting trend of the Proterozoic basement relative to the principal stresses. Structures oriented closest to the mechanically ideal orientation of prevailing stresses will be favored for reactivation (Morley, 2004). Implying that Precambrian structures in

the northern tip of the rift were oriented in a favored orientation to the principal stresses and reactivated in the rifting event. Contrarily, structures in the southern tip were not oriented at favored orientation to the principal stresses and not reactivated.

V. IV Transfers and associated Accommodation zones

As segments flip in polarity from one segment to the other extensional strain is transmitted from one segment to this next through "Accommodation Zones". The primary subdivision of transfer geometry can be divided into two main categories, "synthetic" and "conjugate" systems based on the relative dip direction of consecutive major faults along the rift (Morley et al., 1990, Figure 12). Synthetic is used where the transfer occurs between two faults that dip in the same direction (Figure 12 G-I). On the contrary, conjugate is used to classify a transfer occurring between two faults dipping in the opposite direction (Figure 12 A-F, J). Conjugate is further classified into two types based on whether the two main faults are facing towards each other or away from each other and hence classified as convergent and divergent respectively. Both conjugate and synthetic transfers are further classified based on the locations of the faults relative to each other: approaching, overlapping, collateral, and collinear. An approaching transfer occurs where two fault tips are linked tip to tip and fail to propagate past each other (Figure 12 A, D, G). Overleaping transfers occur when the two faults propagate past each other (Figure 12 B, E, H). Collateral transfers occur where faults run parallel to each other completely overlapping each other (Figure 12 C, F, I) and collinear transfers occur where faults follow a line (Figure 12 J) (Morley et al., 1990). Previous models suggest the formation of various types of accommodation zones based on the transfer (Faulds and Varga, 1998, Rosendahl, 1987, Scott and Rosendahl, 1989, Versfelt and Rosendahl, 1989). Interference accommodation zones (INAZ) are areas where two half-grabens are dipping in the opposite direction inwards. Formed by conjugate convergent transfers (Figure 12 A-C). Isolated accommodation zones (ISAZ) are areas where two half-grabens are dipping in the opposite direction outwards and are

separated by a country rock associated with pre-rifting. This can be formed by conjugate divergent transfers (Figure 12 E-G). Strike-slip accommodation zones (SSAZ) occur in areas where half-grabens flip in polarity within a shared zone. Formed either by conjugate convergent or divergent collinear zone linked through a strike slip fault (Figure 12 J). Last is a synthetic accommodation zone (SAZ) which are areas in between two half-grabens dipping in the same direction. This can be formed through synthetic transfers (Figure 12 G-I).

The only transfer observed from our data is the conjugate convergent overlapping zone. Unlike the typical cross fault rift model (Bosworth, 1985) (figure 13), suggesting the formation of interference accommodation zones with conjugate convergent approaching zone, observation both from surface and subsurface irregular shaped segments in the Malawi rift show along-strike segmentation by changing from half-graben to full-graben geometry linking through interference accommodation zones (Figure 14), and so segments are overlapping and not approaching. Also as observed from SRTM-DEM data all the segments transferred from east to west and no two consecutive segments occurred on the same side hence the possibility of forming a synthetic en echelon was crossed out. Moreover, all the segments dipped inwards toward each other, which was both evident from surface and subsurface data eliminating the possibility of a conjugate divergent overlapping transfer. Finally none of the segments completely overlapped also eliminating the possibility of forming a conjugate convergent collateral transfer. Transfer mode between the eight segments of the rift is identified as a conjugate convergent overlapping transfer linked through interference accommodation zone (Figure 12). Structures observed in the interference accommodation zone display equal displacement of border faults bounding the basin geometry and a symmetric basin geometry in the subsurface. Indicating that the geometry formed by the interference accommodation zone displays a full graben. Smaller normal faults are observed to increase in density as we get to the center of the full graben structure in the subsurface.

If we go back to the evolution of fault linkage, the development of faults can be divided into three stages. First being early linkage, followed by establishment of boundary faults and finally the termination of the fault activity (Morley, 2002). Early linkage of the faults includes the linkage of en echelon faults through synthetic accommodation zones (Morley, 2002). Suggesting the establishment of major boundary faults through linkage of minor fault previously linked through soft linkage at the synthetic accommodation zones and later developing into a hard linkage. Since no en echelon faults are observed in the Malawi rift propagation of border faults along the rift is through hard linkage.

Finally, the Malawi rift appears to terminate against a NW-SE trending Karoo basin which is bounded to the NE by the NW-SE Mwanza fault located in the Shire province (Castaing, 1991). The rift does not continue to the Urema graben as previously suggested (Ring et al., 1992). The Mwanza fault links the southern end of the Malawi rift to the line formed by the basins of the Dombe and the Urema (Chorowicz and Sorlien, 1992). Hence transmitting the rifting of the Malawi to the Urema graben (Casting, 1990). Observations based on the X-derivative map (Figure 8) and topography profiles (Figure 5), suggest that the trend of the rift is clearly been truncated by the Karoo basin. Suggesting that the Malawi rift extends for a total length of ~700 km. As mentioned earlier the Malawi rift is younger and less developed in the South giving a possible explanation for the rift not being able to cut through the Karoo basin.

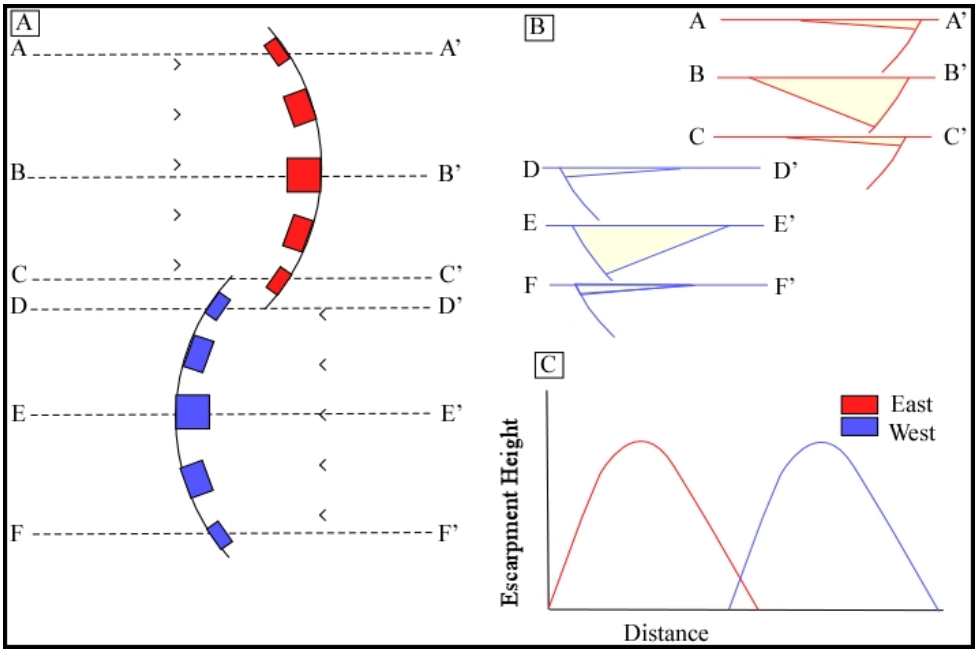

Figure 13: Idealized representation of a segmented and overlapped rift with alternation half-graben polarity. (A) Map view. (B) Idealized cross sections across the rift (note the diminishing of vertical distance on both border faults at the overlap zone). (C) Vertical distance variation of the border faults escarpment.

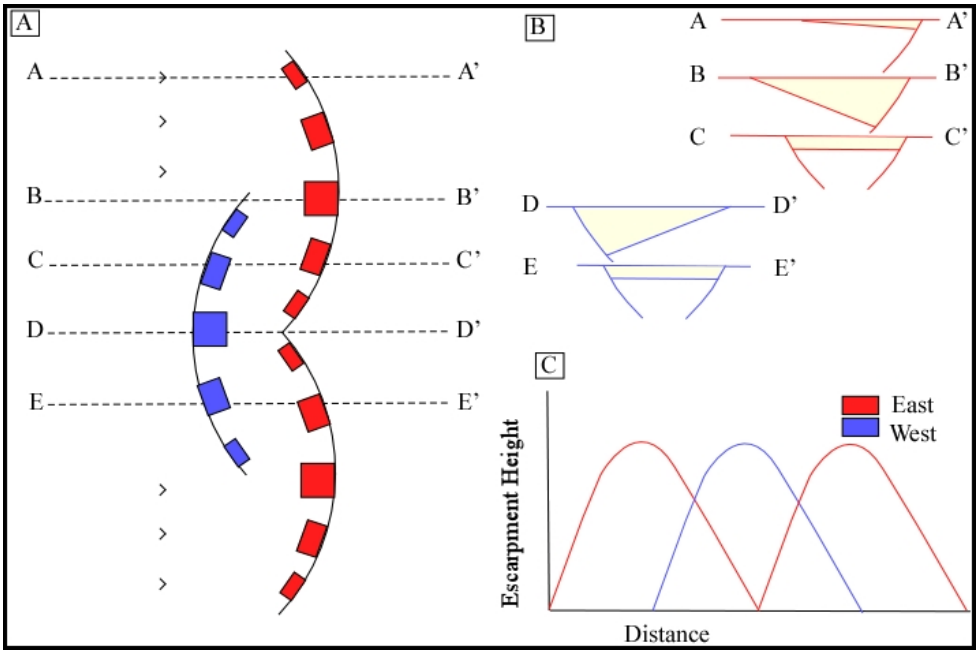

Figure 14: Idealized representation of the presented model for a segmented and overlapped rift with alternation half-graben polarity. Segments shown as half moon for easier comparison with figure 11. (A) Map view. (B) Idealized cross sections across the rift (note the formation of full-grabens at overlap zone). (C) Vertical distance variation of the border faults escarpment.

CHAPTER VI

CONCLUSION

The Malawi rift represents a unique succession of half-graben structures forming the basin architecture of the rift. Half-graben systems don't portray the pattern represented by the cross fault rift model, suggesting half moon curvilinear structures flipping in polarity forming half-grabens interacting tip to tip. However, it shows a pattern of eight half-grabens giving place to the next system of the opposite polarity through interference accommodation zones represented by a full-graben geometry (Figure 16). Portraying the pattern suggested by conjugate convergent overlapping transfer. Location and the orientation of the Karoo grabens (Ruhuhu trough and Maniamba trough) at high angle to the trend of the rift, was proposed as a possible influence on strain localization in those areas preventing the fault from further propagating. Pre-rifting trend of the Proterozoic basement indicate reactivation of these structures or not by the rifting event. Malawi rift terminates against the NW-SE trending Karoo graben forming a total distance of ~700 km.

REFERENCES

Baldridge, S., Olsen, K. and Callendar, .I., 1984. Rio Grande Rift: problems and perspectives. New Mexico Geol. Sot. Guideb., 35th Annu. Conf., pp. 1-12.

Bally, W., 1982. Musings over sedimentary basin evolution. Philos. Trans. R. Sot. London, Ser. A, 305: 325-328.

Biggs, J., Nissen, E., Craig, T., Jackson, J., and Robinson, D. P., 2010. Breaking up the hanging wall of a rift border fault: The 2009 Karonga earthquakes, Malawi. Geophysical Research Letters, 37(11).

Bloomfield, K., 1966. Geological map of Malawi: Zomba, Malawi. Geologic Survey of Malawi, scale 1:1,000,000.

Bosworth, W., 1985. Geometry of propagating continental rifts. Nature, 316(6029), 625-627.

Calais, E., Ebinger, C. J., Hartnady, C., and Nocquet, J. M., 2006. Kinematics of the East African Rift from GPS and earthquake slip vector data. SPECIAL PUBLICATION-GEOLOGICAL SOCIETY OF LONDON, 259, 9.

Cape, C., McGeary, S. and Thompson, G., 1983. Cenozoic normal faulting and the shallow structure of the Rio Grande rift near Socorro, New Mexico. Geol. Sot. Am. Bull., 94(1), 3-14.

Carter, G. S., and Bennett, J. D., 1973. The geology and mineral resources of Malawi (2nd revised edition). Geological Survey of Malawi Bulletin 6, 62.

Castaing, C., 1991. Post-Pan-African tectonic evolution of South Malawi in relation to the Karroo and recent East African rift systems. Tectonophysics, 191(1), 55-73.

Chen, L., and L. Lee, 1992. Progressive generation of control frameworks for image registration, Photo-gramm. Eng. Remote Sens., 58, 1321–1328.

Chenet, P.-Y, and Letouzey, J., 1983. Tectonique de la zone comprise entre Abu Durba et Gebel Mezzazat (Sinai, Egypte) darts le contexte de l'evolution du rift du Suez. Bull. Centres Rech. Explor.-Production Elf Aquitaine, 7(1), 201-215.

Chorowicz, J., 2005. The East African rift system. Journal of African Earth Sciences 43(1), 379-410.

Chorowicz, J., and Sorlien, C., 1992. Oblique extensional tectonics in the Malawi Rift. Geological Society of America Bulletin 104, 1015–1023.

Contreras, J., Anders, M. H., and Scholz, C. H., 2000. Growth of a normal fault system: observations from the Lake Malawi basin of the east African rift. Journal of Structural Geology, 22(2), 159-168.

Crossley, R., and Crow, M. J., 1980. The Malawi rift. Geodynamic evolution of the Afro- Arabian rift system: Accademia Nationale Lincei, 77-87.

Daly, M. C., and Quennell, A. M., 1986. Crustal shear zones and thrust belts: Their geometry and continuity in central africa [and discussion]. Philosophical Transactions of the Royal Society of London. Series A, Mathematical and Physical Sciences, 317(1539), 111-128.

Delvaux, D., 1995. Age of Lake Malawi (Nyasa) and water level fluctuations. Mus R Afr Centr Tervuren (Belg) Dept Geol Min Rapp Ann, 1996(99), 108.

Ebinger, C. J., and M. Casey, 2001. Continental breakup in magmatic provinces: An Ethiopian example, Geology, 29, 527–530.

Ebinger, C., M. Crow, B. Rosendahl, D. Livingstone, and J. Le Fournier, 1984. Structural evolution of the Malawi rift, Africa, Nature, 308, 627-629.

Ebinger, C. J., Deino, A. L., Drake, R. E., and Tesha, A. L. 1989. Chronology of volcanism and rift basin propagation: Rungwe volcanic province, East Africa. Journal of Geophysical Research: Solid Earth 94(B11), 15785-15803.

Ebinger, C.J., Deino, A.L., Tesha, A.L., Becker, T., Ring, U., 1993. Regional control on Rift basin morphology: evolution of the Northern Malawi (Nyassa) Rift. Journal of Geophysical Research 98 (17), 821– 836.

Ebinger, C. J., Rosendahl, B. R., and Reynolds, D. J., 1987. Tectonic model of the Malaŵi rift, Africa. Tectonophysics, 141(1), 215-235.

Faulds, J. E., and Varga, R. J., 1998. The role of accommodation zones and transfer zones in the regional segmentation of extended terranes. SPECIAL PAPERS-GEOLOGICAL SOCIETY OF AMERICA, 1-46.

Flannery, J.W., Rosendahl, B.R., 1990. The seismic stratigraphy of Lake Malawi, Africa: implications for interpreting geological processes in lacustrine rifts. Journal African Earth Sciences 10 (3), 519–548.

Gibbs, A., 1984. Structural evolution of extensional basins. J. Geol. Sot. London, 141(4), 609-620.

Harkin, P.A., 1960. The Rungwe volcanics at the northern end of lake Nyasa. Memoir Geological Survey of Tanganyika 2, 172.

Jackson, J., and Blenkinsop, T., 1997. The Bilila Mtakataka fault in Malaŵi: An active, 100 km long, normal fault segment in thick seismogenic crust. Tectonics, 16(1), 137-150.

Katumwehe, A., 2013. The role of pre-existing structures in the evolution of the Albertine and Rhino grabens in Uganda and Congo. in 2013 GSA annual meeting in Denver.

Modisi, M. P., Atekwana, E. A., Kampunzu, A. B., & Ngwisanyi, T. H., 2000. Rift kinematics during the incipient stages of continental extension: Evidence from the nascent Okavango rift basin, northwest Botswana. Geology, 28(10), 939-942.

Morley, C. K., 1999. Patterns of displacement along large normal faults: implications for basin evolution and fault propagation, based on examples from east Africa. AAPG bulletin, 83(4), 613-634.

Morley, C. K., 2002. Evolution of large normal faults: Evidence from seismic reflection data. AAPG bulletin, 86(6), 961-978.

Morley, C. K., Haranya, C., Phoosongsee, W., Pongwapee, S., Kornsawan, A., and Wonganan, N., 2004. Activation of rift oblique and rift parallel pre-existing fabrics during extension and their effect on deformation style: examples from the rifts of Thailand. Journal of Structural Geology, 26(10), 1803-1829.

Morley, C. K., Nelson, R. A., Patton, T. L., and Munn, S. G., 1990. Transfer Zones in the East African Rift System and Their Relevance to Hydrocarbon Exploration in Rifts (1). AAPG Bulletin, 74(8), 1234-1253.

Ring, U., and Betzler, C., 1995. Geology of the Malawi Rift: kinematic and tectonosedimentary background to the Chiwondo Beds, northern Malawi. Journal of Human Evolution 28(1), 7-21.

Ring, U., Betzler, C., and Delvaux, D., 1992. Normal vs. strike-slip faulting during rift development in East Africa: The Malawi rift. Geology 20(11), 1015-1018.

Rosendahl, B. R., 1987. Architecture of continental rifts with special reference to East Africa. Annual Review of Earth and Planetary Sciences, 15, 445.

Rosendahl, B. R., Kilembe, E., and Kaczmarick, K., 1992. Comparison of the Tanganyika, Malawi, Rukwa and Turkana rift zones from analyses of seismic reflection data. Tectonophysics 213(1), 235-256.

Rosendahl, B., Reynolds, D., Lorber, P., Burgess, C., McGill, J., Scott, D., Lambaise, J. and Derksen, S., 1986. In: L.Frostick (Editors), Sedimentation in the East African Rifts. Geol. Society. London, Spec. Publ. 25, 29-43.

Scott, D. L., and Rosendahl, B. R., 1989. North Viking graben: an east African perspective. AAPG Bulletin, 73(2), 155-165.

Smith, R. and Bruhn, R., 1984. Intraplate extensional tectonics of the eastern Basin-Range: Inferences on structural style from seismic reflection data, regional tectonics, and ther- mal-mechanical models of brittle-ductile deformation. J. Geophys. Res., 89: 5733-5762.

Specht, T. D., and Rosendahl, B. R., 1989. Architecture of the Lake Malawi rift, east Africa. Journal of African Earth Sciences (and the Middle East) 8(2), 355-382.

Stamps, D. S., Calais, E., Saria, E., Hartnady, C., Nocquet, J. M., Ebinger, C. J., and Fernandes, R. M., 2008. A kinematic model for the East African Rift. Geophysical Research Letters, 35(5).

Versfelt, J., and Rosendahl, B. R., 1989. Relationships between pre-rift structure and rift architecture in Lakes Tanganyika and Malawi, East Africa, 354-357.

Zorin, Y., 1981. The Baikal rift: an example of the intrusion of asthenospheric material into the lithosphere as the cause of disruption of lithospheric plates. Tectonophysics, 73: 91-10.

VITA

Haifa Salim Al Salmi

Candidate for the Degree of

Master of Science

Thesis: BORDER FAULTS LINKAGE AND SEGMENTATION ALONG THE MALAWI RIFT

Major Field: Geology

Biographical:

Education:

Completed the requirements for the Master of Science in Geology at Oklahoma State University, Stillwater, Oklahoma in December, 2014.

Completed the requirements for the Bachelor of Engineering in Mechanical at Sultan Qaboos University, Muscat, Sultanate Of Oman in 2011.

Experience:
Road Transport and Compliance Coordinator; 2011-2012; Shell Oman Marketing Company, Muscat, Sultanate Of Oman.

Dhulaima Internship; Summer 2010; Petroleum Development Oman, Muscat, Sultanate Of Oman.